A ^{1}H NMR Study of Human Calcitonin in Solution†

Andrea Motta,*,‡ Piero Andrea Temussi,§ Erich Wünsch,∥ and Günter Bovermann∥,⊥

Istituto per la Chimica di Molecole di Interesse Biologico del CNR, 80072 Arco Felice (Napoli), Italy, Dipartimento di Chimica, Università di Napoli "Federico II", 80134 Napoli, Italy, and Max-Planck-Institut für Biochemie, Abteilung Peptidchemie, D-8033 Martinsried bei München, Federal Republic of Germany

Received February 12, 1990; Revised Manuscript Received October 3, 1990

ABSTRACT: Human calcitonin (hCT) has been investigated by NMR at 400 MHz in $DMSO_{d6}$ and in an 85% $DMSO_{d6}$–15% ^1H_2O (v/v) cryoprotective mixture. All backbone and side-chain resonances have been assigned, and the secondary structure has been determined in both solvents. In $DMSO_{d6}$, the simultaneous presence of $d_{\alpha N}$, d_{NN}, and some specific weak medium-range nuclear Overhauser effects, together with the amide temperature coefficients and the analysis of the NH–αCH spin–spin coupling constants, indicates that hCT is highly flexible but with three domains (comprising segments Asn^3–Gly^{10}, Gln^{14}–Thr^{21}, and Thr^{25}–Ala^{31}) in extended conformations which dynamically transform into isolated β turns in the N- and C-terminal regions and into adjacent tight turns, resembling a 3_{10} helix structure, in the central part. The DMSO–water mixture rigidifies the polypeptide chain, favoring an ordered, extended conformation. NOESY data indicate the presence of a short double-stranded antiparallel β sheet in the central region made by residues 16–21 and connected by a two-residue hairpin loop formed by residues 18 and 19. Two tight turns, formed by residues 3–6 and 28–31, were also identified. The central β sheet does not favor an amphipathic distribution of the residues as found for salmon calcitonin [Motta, A., Castiglione Morelli, M. A., Goud, N., & Temussi, P. A. (1989) *Biochemistry 28*, 7998–8002]. This is in agreement with the smaller tendency of hCT to form the amphipathic α helix, postulated to be responsible for the interaction of hCT with lipids. The possible role of the cis–trans isomerism of Pro is discussed.

Calcitonin (CT)[1] is a peptide hormone of 32 residues that plays a central role in calcium–phosphorus metabolism (Austin & Heath, 1981) and has been postulated to be a neuromodulator and/or a neurotransmitter (Fisher et al., 1981; Rizzo & Goltzman, 1981). It would be desirable to find correlations between these biological functions and structural features, especially since CT finds an ever-increasing use as a drug for various diseases in which it is necessary to favor calcium uptake from the body fluids, notably osteoporosis. A major difficulty in formulating structure–activity relationships resides in the fact that the mechanism of action of CT in calcium uptake is essentially unknown; e.g., it is not even certain whether a specific interaction with a receptor is implicated. Only general hypotheses have been put forward on the possible role of an amphipathic helix (Epand, 1983; Epand et al., 1983; Moe et al., 1983; Moe & Kaiser, 1985) and on the importance of conformational flexibility (Epand et al., 1985, 1986a). A correlation between hypocalcemic activity and the ability to solubilize lipids indicated that, among several C-terminal amidated fragments of sCT, only the 1–23 segment retains both significant hypocalcemic activity and lipid solubilization ability (Epand et al., 1986b). This observation is in agreement with the fact that, among the sequences of several calcitonins (Dayhoff, 1978), the N-terminal 1–10 segment is highly conservative, as would be the case for the message domain of the hormone, but makes it very difficult to explain why hCT is more than 1 order of magnitude less active than sCT (Findlay et al., 1983). A comparison of their primary structures (Scheme I) shows in fact that most of the amino acid substitutions (12 out of 16, lightface in Scheme I) are concentrated in the segment 11–27, which, according to Epand et al. (1986a), should only increase receptor binding when conformational flexibility is slightly increased by amino acid residues with less bulky side chains and less tendency to form helical structure.

Scheme I: Amino Acid Sequence of hCT (h) and sCT (s)[a]

```
                1                   5                  10                  15
h: Cys-Gly-Asn-Leu-Ser-Thr-Cys-Met-Leu-Gly-Thr-Tyr-Thr-Gln-Asp-Phe-
   |____________________|
s: Cys-Ser-Asn-Leu-Ser-Thr-Cys-Val-Leu-Gly- Lys-Leu-Ser- Gln- Glu-Leu-
   |_____________________|
                1                   5                  10                  15

                    20                  25                  30
h: Asn-Lys-Phe-His-Thr-Phe-Pro-Gln-Thr-Ala- Ile- Gly-Val- Gly-Ala- Pro-NH2

s:His-Lys- Leu-Gly-Thr-Tyr-Pro-Arg-Thr-Asn-Thr-Gly-Ser-Gly-Thr-Pro-NH2
                    20                  25                  30
```

[a] Common amino acids are in boldface.

† Dedicated to the memory of Antonio De Marco.

‡ Istituto per la Chimica di Molecole di Interesse Biologico del CNR.

§ Università di Napoli.

∥ Max-Planck-Institut für Biochemie.

⊥ Present address: Sandoz AG, Bau 503/1602 CH 4002 Basel, Switzerland.

[1] Abbreviations: CT, calcitonin; sCT, salmon calcitonin; hCT, human calcitonin; NMR, nuclear magnetic resonance; $DMSO_{d6}$, perdeuterated dimethyl sulfoxide; NOE, nuclear Overhauser enhancement; ppm, parts per million; 1D, one dimensional; 2D, two dimensional; DQF-COSY, two-dimensional double-quantum filtered correlated spectroscopy; relayed COSY, relayed coherence-transfer spectroscopy; TOCSY, total correlation spectroscopy; NOESY, two-dimensional nuclear Overhauser enhancement spectroscopy; T_1, spin–lattice relaxation time; $d_{\alpha N}$, distance between the αCH of residue i and the NH of residue $i + 1$; $d_{\alpha N}(i,i+2)$, distance between the αCH of residue i and the NH of residue $i + 2$; d_{NN}, distance between the NH protons of residues i and $i + 1$; ppb, parts per billion; $^3J_{HN\alpha}$, vicinal coupling constant between NH and α protons; $d_{\alpha N}(i,i+3)$, distance between the αCH of residue i and the NH of residue $i + 3$; $d_{\alpha\beta}(i,i+3)$, distance between the αCH of residue i and the β proton(s) of rese $i + 3$; $d_{\alpha N}(i,i+4)$, distance between the αCH of residue i and the NH of residue $i + 4$; SDS, sodium dodecyl sulfate.

0006-2960/91/0430-2364$02.50/0 © 1991 American Chemical Society

Early NMR studies of hCT in neat $DMSO_{d6}$ and in ^2H_2O (Wüthrich, 1976), indicated that chemical shift data are consistent with a totally random conformation. We recently reported (Motta et al., 1989), however, that the conformation of sCT changes from random to progressively ordered forms when it is transferred from water to DMSO and, particularly, to a cryoprotective mixture (Douzou & Petsko, 1984; Motta et al., 1987, 1988; Fesik & Olejniczak. 1987) at low temperatures.

Here we report an NMR study on hCT aiming at the characterization of its secondary structure in $DMSO_{d6}$ and in DMSO–water mixtures. The latter medium is one of the so-called cryoprotective solvents that have been widely used to investigate several enzyme-catalyzed reactions at low temperatures (Douzou & Petsko, 1984; Fink, 1986; Tobias & Markley, 1986), since such mixtures have properties, at low temperatures, close to those of water at room temperature. By using cryoprotective mixtures, it is possible to reach unusually low temperatures for a polar environment, therefore increasing dramatically the viscosity (Schichman & Amey, 1971) and making the NOEs observable also in medium-sized peptides (Motta et al., 1987, 1988; Fesik & Olejniczak, 1987).

Although hCT in $DMSO_{d6}$ is characterized by considerable conformational flexibility, we observed many NOE connectivities that could be interpreted in terms of well-defined structural domains in equilibrium between two families of conformations. The use of cryosolvents stabilized a single conformation, which seems to be important for the interaction with the membrane.

Materials and Methods

hCT was prepared by classical methods of peptide synthesis in solution (the original scheme will be reported elsewhere).[2]

Sample concentration was usually about 3×10^{-3} M both in $DMSO_{d6}$ and in 85% $DMSO_{d6}$–15% ^1H_2O (v/v). Deuterated solvents originated from Merck Sharp & Dohme Ltd., Canada. Sample tubes were carefully degassed by means of several freeze–thaw cycles, by use of a home-made air-tight device designed by one of us (G.B.) that avoids sealing of the tube and thus makes additions to the solution a very easy procedure.

^1H spectra were recorded at 400 MHz on a Bruker AM-400 spectrometer interfaced to an Aspect 3000 computer and referenced to the residual ^1H–$DMSO_{d6}$ signal, assumed to resonate at 2.50 ppm. 1D spectra sere typically acquired in quadrature detection.

For 2D experiments, namely, DQF-COSY (Piantini et al., 1982), relayed COSY (Eich et al., 1982), TOCSY (Braunschweiler & Ernst, 1983; Bax & Davis, 1985), and NOESY (Macura & Ernst, 1980), the time-proportional phase incrementation scheme was used (Drobny et al., 1979; Bodenhausen et al., 1980). Usually, 512 equally spaced evolution time period t_1 values were acquired, averaging 64–128 transients of 2048 points, with 3600 Hz of spectral width. In order to correct for the different base-line direct-current offsets introduced into t_1 cross sections of the spectrum by errors in the Fourier transform routine, the first block of the data was divided by a factor of 2 before Fourier transformation (Otting et al., 1986). Time domain data matrices were zero filled in ω_1 dimension to 2K and to 8K in ω_2, thus yielding a digital resolution of 3.5 and 0.88 Hz/point, respectively. For representation purposes, 2K × 2K matrices were used throughout; 10°-shifted squared sine-bell window functions were applied before transformation in both dimensions. For NOESY experiments, a series of mixing times (50, 100, 150, and 350 ms) was used in neat $DMSO_{d6}$ for assignment purposes. In cryosolvents we collected experiments with several mixing times, but 250 ms (at 295 K) and 180 ms (at 280 K) proved the best compromise to detect large NOE cross-peaks without spin-diffusion. Irradiation of the ^1H_2O resonance was achieved by coherent irradiation (Zuiderweg et al., 1986) during the relaxation time and, in the case of the NOESY, during the mixing time. Such procedure eliminates t_1-dependent base-line fluctuation leading to a clean spectrum without ω_2 streaks.

The cis–trans exchange rate was estimated at 310 K according to the method proposed by Jeener et al. (1979). For a system exchanging between two sites (cis and trans) the cross-peak amplitude goes through a maximum for:

$$\tau_{mix} = (\ln [(R_1 + k)/R_1])/k \quad (1)$$

k being the exchange-rate constant. Cross-peaks of appreciable intensity can be detected by selecting the temperature such that $k \geq R_1$ (T_1^{-1}) (Jeener et al., 1979). Accordingly, 2D exchange experiments were carried out at 310 K with mixing times ranging between 500 ms and 1 s, in order to achieve cross-peak maximum intensity.

Results

Sequential Assignment and Secondary Structure in Neat $DMSO_{d6}$. The assignment of the hCT spectrum was carried out by using the sequential approach developed by Wüthrich and co-workers (Billeter et al., 1982; Wüthrich et al., 1984). Identification of the complete spin systems of all 32 residues was based on DQF-COSY, relayed-COSY, and TOCSY and complemented with NOESY experiments when ambiguities arose. The identified amino acids were sequentially ordered by resorting to NOEs between backbone protons and compared with the known primary sequence (Wüthrich, 1986). Finally, the NOEs pattern was interpreted in terms of secondary structure elements (Billeter et al., 1982; Wüthrich et al., 1984). Since this process has been described in great detail in the literature for the general case and specifically for sCT (Motta et al., 1989), we shall not repeat the details of the assignment process here. Sequential assignment of hCT in neat $DMSO_{d6}$ was obtained by using the NH–α fingerprint region of a NOESY spectrum at 310 K with 350-ms mixing time (Figure 1). Due to crowding of cross-peaks, only the segment from Phe^{16} to Phe^{22} is explicitly indicated by a continuous path. The NH position of Cys^1 was not detectable, most likely because of the fast exchange with the residual water of $DMSO_{d6}$, but all the $d_{\alpha N}$ connections between adjacent residues from Gly^2 to Phe^{22} were clearly seen. At Pro^{23} the loss of connectivity was inevitable, but the effects between Phe^{22} NH and Pro^{23} δ protons and between Pro^{23} αCH and Gln^{24} NH protons were identified, allowing the sequential relation between sites 22–23 and 23–24. From Gln^{24}, the $d_{\alpha N}$ connectivities could be followed as far as Ala^{31}, whose NOE with the δ protons of Pro^{32} completed the chain. It was therefore possible to assign all resonances to specific protons for each residue of hCT. The complete sequence-specific assignment of resonances is reported in Table I.

Weak $d_{\alpha N}(i,i+2)$ medium-range effects are also present in Figure 1 (boxed cross-peaks). They indicate connections between Gln^{14} and Phe^{16}, Phe^{16} and Lys^{18}, and Phe^{19} and Thr^{21} and are suggestive of a 3_{10}-helical character (see below).

Figure 2 shows the NOESY diagonal d_{NN} region of hCT in neat $DMSO_{d6}$ at 310 K. Surprisingly, it was possible to

[2] A preliminary communication on the synthesis has been presented by G. Wendlberger and E. Wünsch at the 4th Weygand-Scoffone Conference, 1988, San Vito di Cadore, Italy.

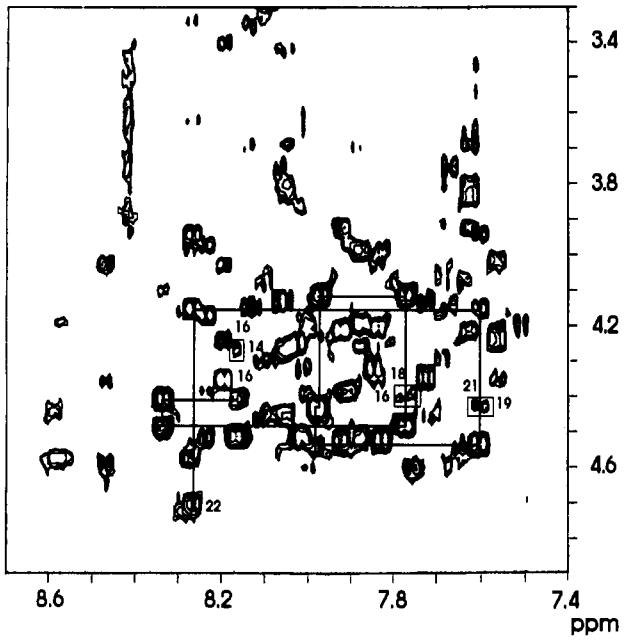

FIGURE 1: Backbone fingerprint region of a phase-sensitive NOESY spectrum (350-ms mixing time) of hCT in neat $DMSO_{d6}$ at 310 K. The assignment of the residues was obtained by connecting COSY peak positions to NOESY cross-peaks manifesting the connectivity to the following residue in the sequence, as explicitly indicated by a continuous path for the segment from Phe^{16} to Phe^{22}. Boxes are drawn around connectivities that represent $d_{\alpha N}(i,i+2)$ medium-range effects, suggestive of a 3_{10}-helical character (see text).

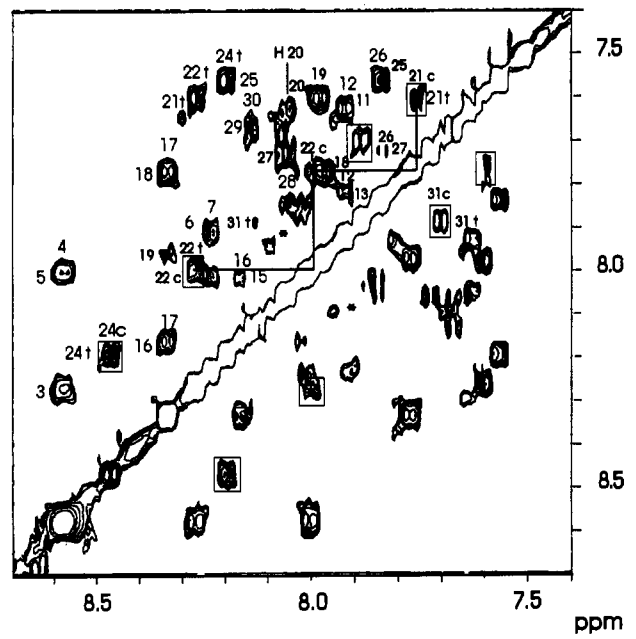

FIGURE 2: Amide NH region of NOESY spectrum (τ_m = 350 ms) of hCT in neat $DMSO_{d6}$ at 310 K. Observed connectivities are all labeled with the site number followed by a t or a c referring to trans (major) and cis (minor) forms, when ambiguity arose. Boxes identifying exchange cross-peaks for Thr^{21}, Phe^{22} (connected by a solid-line pathway), and Gln^{24} due to Pro^{23} cis–trans isomerism and for Ala^{31} due to Pro^{32} isomerism. They were observed in a 700-ms mixing time NOESY and superimposed on the original 350-ms mixing time NOESY spectrum. H20 indicates connection between 2H, at low field, and 4H of His^{20} ring. Asterisk marks an impurity.

detect strong cross-peaks along virtually the entire length of the molecule. Namely, the absence of cross-peaks was noted in the Cys^1–Asn^3 and Thr^{13}–Asp^{15} segments, thus identifying definite regions. This finding is well supported by amide temperature coefficients (Figure 3), which unveil the presence

Table I: ^1H Chemical Shift of hCT in $DMSO_{d6}$ at 310 K[a]

residue	shift of proton resonance (ppm) NH	αH	βH	others
C^1		3.91	3.15; 2.96	
G^2	8.05	3.79; 3.57		
N^3	8.27	4.56	2.85; 2.61	δNH_2 7.35; 6.90
L^4	8.58	4.20	1.68; 1.55	γCH 1.62
				δCH_3 0.87; 0.83
S^5	8.01	4.39	3.69; 3.69	γOH 4.97
T^6	7.91	4.17	3.98	γOH 4.89
				γCH_3 1.08
C^7	8.24	4.52	3.13; 2.89	
M^8	8.02	4.32	1.95; 1.83	γCH_2 2.43; 2.43
				ϵCH_3 2.12
L^9	7.86	4.27	1.52; 1.49	γCH 1.62
				δCH_3 0.86; 0.83
G^{10}	8.06	3.81; 3.61		
T^{11}	7.64	4.22	3.93	γOH 4.79
				γCH_3 0.94
Y^{12}	7.93	4.52	2.98; 2.75	2,6H 7.04
				3,5H 7.63
T^{13}	7.84	4.20	3.99	γOH 4.88
				γCH_3 1.02
Q^{14}	7.89	4.25	1.88; 1.75	γCH_2 2.09; 2.01
				δNH_2 7.20; 6.73
D^{15}	8.03	4.51	2.58; 2.42	
F^{16}	8.17	4.41	3.06; 2.83	2,6H 7.26
				3,5H 7.21
				4H 7.23
N^{17}	8.34	4.48	2.82; 2.54	δNH_2 7.52; 6.93
K^{18}	7.78	4.12	1.59; 1.47	γCH_2 1.26; 1.26
				δCH_2 1.32; 1.32
				ϵCH_2 2.74; 2.74
				ϵNH_2 7.60
F^{19}	7.98	4.43	3.02; 2.82	2,6H 7.23
				3.5H 7.27
				4H 7.23
H^{20}	7.99	4.53	2.99; 2.91	2H 8.05
				4H 7.62
T^{21}	7.62t	4.16t	3.96t	γOH 4.92
				γCH_3t 0.95
	7.74c	4.09c	3.87c	γCH_3c 0.99
F^{22}	8.27t	4.70t	3.03t; 2.84t	2,6H 7.25
				3,5H 7.25
				4H 7.27
	8.00c	4.60c	2.87c; 2.54c	
P^{23}		4.36t	2.06t; 2.02t	γCH_2t 1.85; 1.85
				δCH_2t 3.63; 3.40
		4.32c	2.09c; 1.90c	γCH_2c 1.85; 1.85
				δCH_2c 3.54; 3.38
Q^{24}	8.20t	4.24t	1.88t; 1.81t	γCH_2t 2.17; 1.94
				δNH_2 7.29; 6.80
	8.46c	4.36c	2.01c; 1.80c	γCH_2c 2.21; 1.99
$T^{2}15$	7.58	4.21	4.02	γOH 5.01
				γCH_3 1.04
A^{26}	7.85	4.35	1.22	
I^{27}	7.74	4.13	1.72	γCH_2 1.44; 1.09
				γCH_3 0.84
				δCH_3 0.88
G^{28}	8.06	3.83; 3.57		
V^{29}	7.69	4.15	1.97	γCH_3 0.88; 0.88
G^{30}	8.14	3.71; 3.69		
A^{31}	7.90t	4.53t	1.20t	
	7.70c	4.30c	1.16c	
P^{32}		4.22t	2.10t; 1.79t	γCH_2t 1.86; 1.80
				δCH_2t 3.59; 3.56
		4.18c	1.85c; 1.73c	γCH_2c 1.80; 1.71
				δCH_2c 3.51; 3.47
				NH_2 7.73; 7.65

[a] c and t refer to cis and trans, respectively.

of a third region, as suggested by the grouping in three segments corresponding to Asn^3–Gly^{10}, Gln^{14}–Thr^{21}, and Thr^{25}–Ala^{31} regions. None of the temperature coefficients is close enough to zero (Figure 3) to indicate the presence of stable hydrogen bonds in conformationally defined regions throughout the temperature range examined (Smith & Pease,

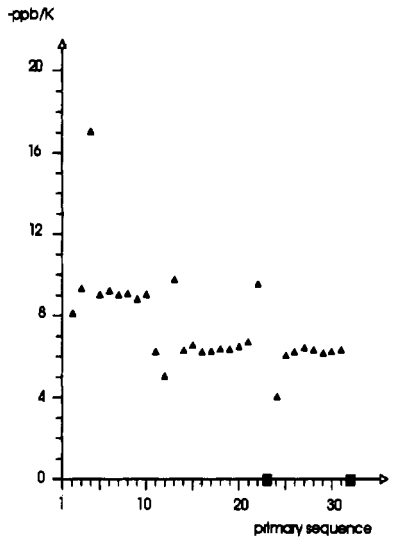

FIGURE 3: Amide temperature coefficients of hCT in neat $DMSO_{d6}$ reported as (−ppb/K) values vs amino acidic composition of the hormone. For half of the resonances, well-enough resolved to allow a direct determination of their temperature dependence, 1D spectra in the range 295–320 K were used. The remaining coefficients were determined from NOESY spectra recorded at 300, 310, and 320 K. Full squares in the abscissa symbolize Pro residues at sites 23 and 32, which lack amide protons.

1980). On the other hand, most unstructured, flexible peptides in $DMSO_{d6}$ show NH temperature coefficients in the range 4.0–5.5 ppb/K (our unpublished observations). That is, coefficients that fall in this range are typical of solvent-exposed NHs, whereas smaller coefficients indicate protons not accessible to solvent molecules. For higher values, as in our case with all values larger than 6 ppb/K (Figure 3), it is fair to assume that we are observing an exchange between a (labile) hydrogen-bond status and a more disordered (solvent exposed) status. In addition, it is also possible that some of the very large coefficients, such as those of the first 10 residues, reflect a relative reorientation of the NH with respect to the adjacent carbonyl group (Llinás & Klein, 1975), due to a conformational transition between a structured domain and more extended conformations. This would be in agreement with the contemporary presence of strong $d_{\alpha N}$ (Figure 1) and strong d_{NN} (Figure 2) effects and the weak medium-range $d_{\alpha N}(i,i+2)$ NOEs (boxed cross-peaks in Figure 1). It is well established that it is typical for a polypeptide backbone in an extended conformation that the sequential d_{NN} NOEs are very weak or absent and that the sequential $d_{\alpha N}$ NOEs are very strong, with $^3J_{HN\alpha}$ greater than 8 Hz (Wüthrich et al., 1984; Pardi et al., 1984). On the contrary, helices are characterized by strong sequential d_{NN} NOEs in combination with relatively weak $d_{\alpha N}$ NOEs and medium-range $d_{\alpha N}(i,i+3)$, $d_{\alpha\beta}(i,i+3)$, and $d_{\alpha N}(i,i+4)$ for the α type and, in addition, $d_{\alpha N}(i,i+2)$ for the 3_{10} type, with small values (<4 Hz) of $^3J_{HN\alpha}$ for both of them (Wagner et al., 1986; Wüthrich, 1986). According to the above data, the three distinct domains, most likely comprising the segments Asn^3–Gly^{10}, Gln^{14}–Thr^{21}, and Thr^{25}–Ala^{31}, are neither in a single conformation nor in a random distribution of families but are characterized by a significant population of extended conformations which dynamically transform into isolated β turns, especially in the N- and C-terminal parts, and into adjacent turns in the central part of the hormone. In particular, the presence of weak medium-range NOEs in the Gln^{14}–Thr^{21} region strongly suggests the presence of a 3_{10}-helix-like structure (Wagner et al., 1986) in $DMSO_{d6}$ solution. Such a dynamic averaging is also expected to lower the observed $^3J_{HN\alpha}$ coupling constants for the extended form and to increase them for the helical one. According, we found that the coupling constants for the segments are averaged to a value of 6.0 Hz.

Interestingly, in $DMSO_{d6}$ we found evidence for the presence of isomers with cis peptide bonds for the prolyl residues at sites 23 and 32 (25% of cis isomer at 295 K). For Pro^{23}, it was revealed by an NOE effect between the αCH protons of Phe^{22} and Pro^{23}. An α–α NOE cross-peak between Ala^{31} and Pro^{32} confirmed the cis isomer for Pro^{32}. The presence of discrete major and minor resonances suggests that the two forms interchange slowly on the NMR time scale (Dwek, 1973). Examination of the temperature dependence of the hCT spectrum revealed an entirely reversible increase in the relative intensity of the minor resonances as the temperature was raised. At 310 K, we were able to detect exchange connectivities for Thr^{21}, Phe^{22}, Gln^{24}, and Ala^{31} resonances. An example of unambiguous evidence that the two species are in equilibrium in solution is given in Figure 2. Boxes identify exchange cross-peaks, observed with 700-ms mixing time, connecting the two spectral positions relative to Thr^{21}, Phe^{22}, Gln^{24}, and Ala^{31} amide resonances. They were superimposed on the 350-ms NOESY used for assignment. According to the method proposed by Jeener et al. (1979), we looked for the maximum intensity of the exchange cross-peaks at 310 K by varying the mixing time of NOESY experiments (see Materials and Methods). A plot of cross-peak intensity vs mixing time presented a maximum for 810 ms. Spin–lattice relaxation times were measured by selective inversion recovery for the δ protons of both Pro^{23} isoforms. Although they resonate in a crowded region, we measured values for them homogeneous within experimental error (1.2 s). According to the found experimental parameters, from eq 1 a value of 9.0×10^{-1} s^{-1} could be estimated for the rate of transfer at 310 K from one form of the hormone to the other. Such a value confirms the slow rate of interconversion and is similar to the reported values for proline isomerism in proteins (Brandts et al., 1975; Schmid & Baldwin, 1978).

Except for the resonances sensitive to the geometry of the prolyl imides bonds of Pro^{23} [those stemming from Thr^{21}, Phe^{22}, Pro^{23}, Gln^{24} (Table I)] and Pro^{32} [those of Ala^{31} and Pro^{32} (Table I)], all resonances of the remaining residues appeared to be in a homogeneous state, as suggested by the single chemical shift value for each proton and by the above exchange cross-peaks. Sequence-specific assignment may be useful to clarify this issue. In Figure 2, a separate pathway of NOE connectivities for the minor form could be identified between Thr^{21} and Phe^{22} (solid-line pathway connecting boxed cross-peaks 21c and 22c). Lacking amide proton, Pro^{23} prevented connection for the minor form up to Gln^{24}. All the other cross-peaks in Figure 2 (labeled with the site number followed by a t when ambiguity arose) stem from the major form of the hormone. In fact, the complete assignment pathway could be followed with few interruptions (see above). Accordingly, the global conformations of the two forms are very similar.

The existence of two isoforms slowly interchanging has also been reported for calbindin D_{9k}, a 75 amino acid protein. Analysis of proton–proton NOEs along the protein backbone, as well as the presence of alternative connectivity pathways in the amide region, provided unambiguous evidence that the two forms of the folded protein differ only in the isomerization state of the peptide bond of Pro^{43} (Chazin et al., 1989; Kördel et al., 1990).

Secondary Structure in DMSO–Water Cryosolvent. hCT was also studied in an 85% $DMSO_{d6}$–15% ^1H_2O (v/v) mixture

Table II: ^1H Chemical Shifts of hCT in 85% $DMSO_{d6}$–15% ^1H_2O (v/v) at 280 K[a]

residue	shift of proton resonance (ppm)			
	NH	αH	βH	others
C^1		4.03	3.20; 3.04	
G^2	8.10	3.67; 3.49		
N^3	8.25	4.64	2.79; 2.65	δNH_2 7.45; 7.02
L^4	8.63	4.29	1.58; 1.50	γCH 1.58
				δCH_3 0.85; 0.81
S^5	8.09	4.20	3.53; 3.48	γOH 4.93
T^6	7.96	4.11	3.91	γOH 4.80
				γCH_3 1.02
C^7	8.04	4.41	3.03; 2.99	
M^8	7.82	4.23	2.15; 1.93	γCH_2 2.31; 2.31
				ϵCH_3 2.07
L^9	7.93	4.21	1.47; 1.38	γCH 1.48
				δCH_3 0.86; 0.86
G^{10}	8.00	3.71; 3.64		
T^{11}	7.85	4.15	3.99	γOH 4.89
				γCH_3 0.90
Y^{12}	7.78	4.59	2.83; 2.64	2,6H 7.12
				3,5H 7.68
T^{13}	8.14	4.55	4.38	γOH 4.96
				γCH_3 1.12
Q^{14}	7.96	4.36	1.86; 1.79	γCH_2 2.09; 2.06
				δNH_2 7.29; 6.67
D^{15}	8.31	4.40	2.81; 2.63	
F^{16}	8.24	4.52	3.26; 2.95	2,6H 7.26
				3,5H 7.25
				4H 7.28
N^{17}	8.43	4.63	2.75; 2.62	δNH_2 7.18; 6.99
K^{18}	7.82	4.36	1.68; 1.49	γCH_2 1.30; 1.30
				δCH_2 1.28; 1.28
				ϵCH_2 2.70; 2.70
				ϵNH_2 7.62
F^{19}	8.02	4.10	3.21; 3.03	2,6H 7.28
				3,5H 7.23
				4H 7.23
H^{20}	8.27	4.42	2.89; 2.82	2H 8.26
				4H 7.41
T^{21}	8.02t	4.24t	3.98t	γOH 4.94
				γCH_3t 1.05
	7.87c	4.14c	3.81c	γCH_3c 0.96
F^{22}	8.28t	4.73t	3.18t; 3.04t	2,6H 7.26
				3,5H 7.28
				4H 7.27
	8.54c	4.61c	2.98c; 2.62c	
P^{23}		4.38	2.14; 2.08	γCH_2 1.88; 1.88
				δCH_2 3.60; 3.48
Q^{24}	8.38	4.12	1.94; 1.89	γCH_2 2.25; 2.06
				δNH_2 7.39; 6.92
T^{25}	7.69	4.15	3.90	γCH 5.02
				γCH_3 1.01
A^{26}	7.88	4.36	1.28	
I^{27}	7.93	4.29	1.68	γCH_2 1.33; 1.18
				γCH_3 0.86
				δCH_3 0.89
G^{28}	7.98	3.88; 3.68		
V^{29}	7.86	4.24	1.91	γCH_3 0.88; 0.88
G^{30}	8.21	3.72; 3.66		
A^{31}	7.85	4.38	1.16	
P^{32}		4.52	2.08; 1.82	γCH_2 1.87; 1.82
				δCH_2 3.71; 3.62

[a] c and t refer to cis and trans, respectively.

at 295 and 280 K. The experimental conditions were chosen by observing the increase of the half-height line width of the spectral lines vs temperature, bearing in mind that the increased viscosity could bring about spin-diffusion effects in NOESY experiments with long mixing times. A temperature setting of 280 K and a mixing time of 180 ms proved the best compromise to detect large NOE cross-peaks without spin-diffusion. Under these new experimental conditions, all resonances needed to be reassigned because one-to-one resonance comparison between the two solvents was not possible. The chemical shifts of the assigned resonances are listed in Table II. Unlike $DMSO_{d6}$, sequential assignment was achieved via the strong $d_{\alpha N}$ connectivities, because the number of the d_{NN} cross-peaks was notably reduced on going from $DMSO_{d6}$ to cryosolvent at 280 K. Figure 4 shows the amide diagonal region of hCT in crysolvent at 280 K of a NOESY with 180-ms mixing time. The reduction of the cross-peaks is evident if compared with the corresponding region in neat $DMSO_{d6}$ (Figure 2). According to the observed NOE pattern, the secondary structure identification procedure (Wagner et al., 1986) indicates that, on going from $DMSO_{d6}$ to cryosolvent, the equilibrium moves toward the extended conformation. Accordingly, we found that the majority of the residues shows coupling constants $^3J_{HN\alpha} > 7$ Hz, as expected for extended structures (Wüthrich, 1986). Furthermore, the small medium-range NOEs and the exchange connectivities observed in $DMSO_{d6}$ (Figure 1) disappeared from the spectra (Figure 5A). Thus, the increased viscosity of the medium brought about by cryomixtures and by lowering of temperature (Schichman & Amey, 1975; Motta et al., 1987) "forces" the hormone into an ordered, extended conformation.

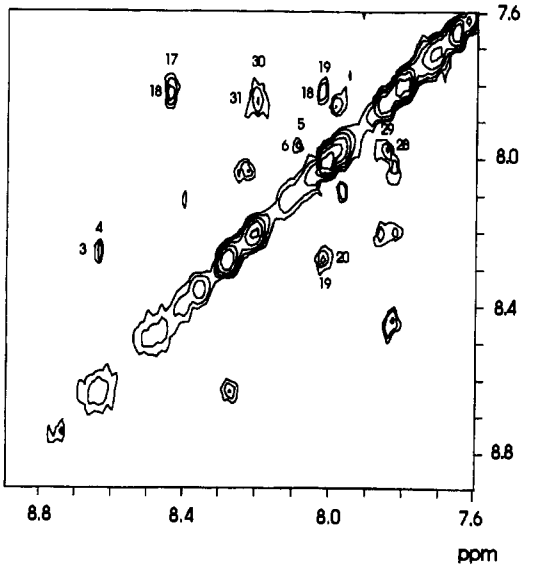

FIGURE 4: Spectral region of the NOESY (τ_m = 180 ms) of hCT in 85% $DMSO_{d6}$–15% ^1H_2O (v/v) at 280 K, showing the d_{NN} connectivities. Cross-peaks are labeled with their sequence numbers.

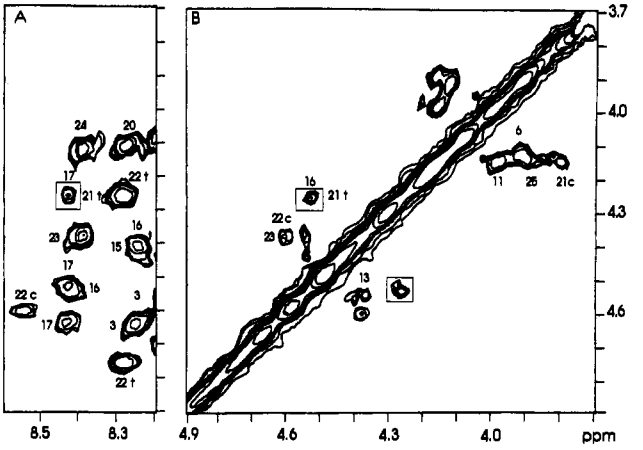

FIGURE 5: NOESY (τ_m = 180 ms) spectral regions of hCT in 85% $DMSO_{d6}$–15% ^1H_2O (v/v) at 280 K. (A) Partial (ω_1 = 3.7–4.9 ppm; ω_2 = 8.2–8.6 ppm) fingerprint region showing sequential $d_{\alpha N}$ NOEs labeled by sequence numbers followed by t (trans) or c (cis). The long-range NOE between the amide of Asn^{17} and the α proton of Thr^{21} is framed. (B) Region (ω_1 = ω_2 = 3.7–4.9 ppm) containing both intraresidue connectivities αH–βH for Thr and interresidue αH–αH. The α–α effect between residues 16 and 21 is boxed.

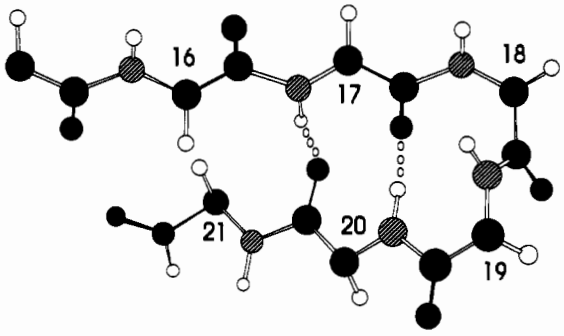

FIGURE 6: Schematic representation of the β-sheet secondary structure for hCT in 85% $DMSO_{d6}$–15% ^1H_2O (v/v), at 280 K as determined by NMR. For each residue the backbone atoms are drawn, and the α protons position is given. Small circles represent hydrogen bonds.

Regarding the location of secondary structure elements, some long-range NOEs, involving the backbone protons, were observed, and their assignment is reported in Figure 5. The NOE between the α protons of Phe^{16} and Thr^{21} (Figure 5B) shows that such residues form an antiparallel β sheet (Wüthrich et al., 1984). The long-range NOE between the amide of Asn^{17} and the α proton of Thr^{21} (boxed cross-peaks in Figure 5A) is consistent with this structure. Such a β sheet requires a hairpin connection between the adjacent antiparallel β strands (Richardson, 1981). The loop could be identified by d_{NN} connectivities in the region 17–20 in the NOESY of Figure 4. The NOEs reported in Figure 5 imply that the hydrogen bonds are between the amides of Asn^{17} and His^{20} and the carbonyl oxygens of His^{20} and Asn^{17}, respectively. All the observed NOEs point to the conclusion that the extended polypeptide assumes, in DMSO–water mixture, a short double-stranded antiparallel β-sheet structure in the central region, linked by a two-residue type I hairpin turn. This structure is shown schematically in Figure 6. In particular, the presence of the Lys^{18}–Phe^{19} d_{NN} connectivity (Figure 4) allows discrimination between type I and type II turns. Two β turns formed by residues 3–6 and 28–31 were also identified through $d_{\alpha N}$ and d_{NN} connectivities.

We also gathered evidences for the presence of an isomer (25%) with a cis peptide bond only at Pro^{23}. In fact, we observed an NOE effect between the α protons of Phe^{22} and Pro^{23} (Figure 5B), as in $DMSO_{d6}$ (see above). No such effect was observed for Ala^{31} and Pro^{32}, thus excluding the presence of a sizable fraction of cis isomer for Pro^{32}. Accordingly, doubling of the resonances was only observed for Thr^{21} and Phe^{22}. Similar results were found for the two conserved prolines of sCT (Scheme I) in 90% $DMSO_{d6}$–10% ^1H_2O (v/v), for which we observed a comparable amount of cis isomer (21%) for Pro^{23} but not for Pro^{32}, which was found to be totally in the trans state (Motta et al., 1989).

Discussion

In this paper we have analyzed the secondary structure of hCT in neat $DMSO_{d6}$ and in an 85% $DMSO_{d6}$–15% ^1H_2O (v/v) cryoprotective mixture. All resonances have been identified and assigned to specific residues by the sequential method. In both solvents we observed large negative NOEs which allowed sequential assignment. In particular, in neat $DMSO_{d6}$, the simultaneous presence of $d_{\alpha N}$ and d_{NN} connectivities, together with some weak medium-range effects in the Gln^{14}–Thr^{21} region (Figures 1 and 2) and the amide temperature coefficients (Figure 3), showed a clear partition into three well-defined regions, namely, Asn^3–Gly^{10}, Gln^{14}–Thr^{21}, and Thr^{25}–Ala^{31}. According to the established qualitative pattern recognition approach, such findings do not yield unambiguous evidence for a particular secondary structure type. They suggest that hCT in neat $DMSO_{d6}$ is neither in a single conformation nor in a mixture of randomly distributed chain but adopts a significant population of extended conformations which dynamically transform into isolated β turns, especially in the N- and C-terminal parts, and consecutive ones in the central region. In particular, the presence of weak $d_{\alpha N}(i,i+2)$ medium-range effects between Gln^{14} and Phe^{16}, Phe^{16} and Lys^{18}, and Phe^{19} and The^{21} (boxed cross-peaks in Figure 1) indicates a helix-like conformation, close to a 3_{10} helix structure in the central part. Such a conclusion is not unusual since distance constraints in tight turns are similar to those in helical peptide segments. For turns of type I and I′ both the sequential and medium-range proton distances coincide closely with those in the 3_{10} helix, and for turns II and II′ qualitative differences from the 3_{10} helix prevail only for the sequential distances $d_{\alpha N}$ and d_{NN} between the second and the third residue of the turn (Wüthrich, 1986). Furthermore, the dynamic process brings about an averaging of the $^3J_{HN\alpha}$ coupling constant to a value of 6.0 Hz, which is between the values expected for the helical and the extended forms.

Similar dynamic averaging has been invoked by Chazin et al. (1988) to interpret the NMR data for the ends of two helical regions of human 3a anaphylatoxin. For those regions they found the simultaneous presence of $d_{\alpha N}$ and d_{NN} NOESY effects, with a corresponding increase of the coupling contants with respect to the α-helix value, and concluded that the two helices appear to fray open. The contemporary presence of $d_{\alpha N}$ and d_{NN} effects has also been reported by Otting et al. (1988) for the chain terminal segments of the *Antennapedia* homeodomain. Such a presence has been interpreted as evidence for high flexibility.

The fast conformational exchange observed in neat $DMSO_{d6}$ at 310 K can be efficiently slowed down in 85% $DMDO_{d6}$–15% ^1H_2O at 280 K. One advantage of these mixtures is the similarity, at low temperature, of their dielectric constants to that of water at room temperature (Douzou & Petsko, 1984), whereas the viscosity is sizably higher [ca. 6 cP at 280 K compared with ca. 1 cP for water at room temperature (Schichman & Amey, 1971)]. The use of these cryoprotective mixtures was motivated, in part, by the possibility of simulating the medium at the interface between bulk water and membrane (Motta et al., 1988). The membrane surface is not a homogeneous solvent environment but rather a highly anisotropic system with a spatially segregated gradient of polarity from water to hydrocarbon. However, under our experimental conditions (low temperature, high viscosity, and reduced hydrogen-bonding capability toward the polypeptide), the hormone is in an environment which may resemble that of the interface between the membrane and the transport fluid, when the flexible polypeptide starts to assume some preferential conformation(s) (Sargent & Schwyzer, 1986). As a partial support to this hypothesis, we have reported (Motta et al., 1989) that a highly flexible polypeptide such as sCT in water adopts a short double-stranded β-sheet structure in 90% $DMSO_{d6}$–10% ^1H_2O (v/v). This structure recalls that characterizing the first step of the model for interaction of a protein signal sequence with a membrane (Briggs et al., 1986; Briggs & Gierasch, 1986). According to this model, a β structure is needed for the interaction with a membrane surface, successively transforming into a helical conformation in the hydrophobic environment of the membrane.

For hCT in an 85% $DMSO_{d6}$–15% ^1H_2O (v/v) cryomixture, we observed only strong $d_{\alpha N}$ effects (Figure 5A) throughout the polypeptide chain, but few weak d_{NN} effects (Figure 4).

Furthermore, two long-range NOE effects between the α protons of Phe[16] and Thr[21] and between the amide of Asn[17] and the α proton of Thr[21] (Figure 5) were also observed. According to the NOE pattern, we propose that, in the DMSO–water mixture, hCT adopts a short double-stranded antiparallel β sheet in the region of residues 16–21, with a two-residue hairpin loop connection made by residues Lys[18] and Phe[19] (Figure 6), and forms two β turns made by residues 3–6 and 28–31. Such structural features, reminiscent of those found for sCT in identical experimental conditions, may be relevant for the interaction of the hormone with the membrane. The amphipathic distribution brought about by the β sheet in sCT (Ser[13], Glu[15], and His[17] are above while Leu[12], Gln[14], and Leu[16] are below the plane) can be the precursor of the amphipathic α helix (Motta et al., 1989), postulated to be responsible for the interaction of sCT with the lipids (Epand et al., 1988).

In hCT, the central β sheet locates Phe[16], Lys[18], and His[20] above the sheet, while Asn[17], Phe[19], and Thr[21] side chains are below it. By examining the nature of the residues, we notice that Phe[16], a nonpolar residue, is together with Lys[18] and His[20], two charged polar residues. On the other hand, Asn[17] and Thr[21], two polar but neutral side chains, are together with Phe[19], a nonpolar one. It is evident that the partition imposed by the β sheet is not amphipathic, but this is in agreement with the fact that hCT has a somewhat smaller tendency than sCT to be amphipathic when folding into an α helix (Epand et al., 1983). The formation of the amphipathic helix in hCT is less probable than in sCT, due to the presence of Asp[15] in the hydrophobic side of the potential helix. As suggested by Epand et al. (1983), perhaps hCT must form a more distorted helix with respect to sCT in order to be amphipathic in the presence of lipids (Epand et al., 1983).

Recently, Doi et al. (1989) have reported that the Leu[9]–Thr[21] region of hCT, in a mixture of 60% water and 40% trifluoroethanol, exists in an amphipathic helical structure.

Evidence for cis–trans isomerism around Xxx–Pro bonds has been found both in $DMSO_{d6}$ and in cryosolvents. In $DMSO_{d6}$ both prolines show considerable amounts of cis isomers. Complete sequence-specific assignment allowed identification of one additional set of minor resonances for Thr[21], Phe[22], Pro[23], Gln[24], Ala[31], and Pro[32] (Table I). They were correlated to the nature of the peptide bond between Phe[22] and Pro[23] and between Ala[31] and Pro[32] by NOESY data. For the major form, cross-peaks were observed between the α protons of Phe[22] and the δ protons of Pro[23] and between the Ala[31] α and the Pro[32] δ protons, typical of a trans peptide in extended conformation. On the contrary, the minor form showed cross-peaks between the α protons of Phe[22] and Pro[23] and between those of Ala[31] and Pro[32], indicating the presence of a cis peptide bond between those amino acid pairs (Wüthrich et al., 1984). Such a presence implies that the two species in solution are in slow equilibrium on the NMR time scale. This was confirmed by the chemical exchange experiments. In Figure 2, squares identify exchange cross-peaks that arise from amide protons that resonate at the frequency of one form in the first dimension, undergo chemical exchange during the mixing period of the experiment, and resonate at the amide frequency of the other form in the second dimension. Those cross-peaks were observed in a 700-ms mixing time NOESY experiment and superimposed on the 350-ms NOESY used for assignment. Similar exchange cross-peaks have also been observed for sCT in aqueous SDS with a peptide:SDS ratio of 1:120 (A. Motta, N. A. Goud, M. A. Castiglione Morelli, and P. A. Temussi, unpublished results). They were unequivocally identified by their sign, identical with that of the diagonal resonances (Davis & Bax, 1985), in a rotating-frame Overhauser experiment. The above observations indicate that the global conformations of the two forms in solution are very similar, with perturbations localized around Pro sites.

Local perturbations have also been invoked for calbindin D_{9k}, even though a relatively larger percentage of residues presents doubling of resonances. Such an effect is attributed to reorganization of the side-chain packing (Chazin et al., 1989).

For hCT, resonance doubling is only induced in residues adjacent to a Pro, with a cis percentage similar to that observed for nonterminal and C-terminal proline in linear oligopeptides (Grathwhol & Wüthrich, 1981). However, if compared with model peptides, a faster cis–trans interconversion rate (9.0×10^{-1} s^{-1} at 310 K) was measured for hCT in $DMSO_{d6}$. This is most likely due to the chain length and the size of the polypeptide, since cis–trans equilibrium has been reported to be coupled with the overall molecular conformation (Hetzel & Wüthrich, 1979). Accordingly, the slow rate of interconversion we observe is closer to the values generally accepted for proline isomerism in proteins (Brandts et al., 1975) than to those found in small model peptides (Grathwhol & Wüthrich, 1981).

In cryosolvent, cis–trans isomerism is only observed for Pro[23] and not for Pro[32], which appears to be predominantly trans. Similar findings have also been reported for sCT in identical experimental conditions (Motta et al., 1989) and in aqueous SDS (at 313 K) with a peptide:SDS ratio of 1:120 (A. Motta, N. A. Goud, M. A. Castiglione Morelli, and P. A. Temussi, unpublished results), i.e., in experimental conditions that favor intramolecular hydrogen bonding and rigidify the peptide structure (Gierasch et al., 1982). The persistence of structural perturbations induced in different solvent media by Pro[23] can be justified by local effects. It is interesting to recall that the half-life for Xxx-Pro isomerization is highly dependent on the peptide chain, and thus on the chemical properties of the site in which the bond is found (Brandl & Deber, 1986). This may explain the difference between Pro[23], always undergoing cis–trans isomerism, and Pro[32], thus hinting at a specific role for Pro[23] in calcitonins. Indirect support to this point comes from the data of Lolkema et al. (1988). They reported that replacement of Pro[327] in the *lac* permease of *Escherichia coli* does not alter permease activity, demonstrating that there is no relationship between permease activity and helix capability of the residue at site 327. They suggested that primarily a chemical property of the side chain at position 327 is important for activity, thus refusing the hypothesis that cis–trans isomerism of Xxx-Pro may provide a mechanism for gating of channels formed by membrane proteins (Brandl & Deber, 1986).

The possible significance of the local effect will be addressed in a separate paper.

Acknowledgments

P.A.T. thanks the Max Planck Geselshaft for the generous hospitality at the M.P.I. of Martinsried, where this work was initiated. We are greatful to a referee for many constructive criticisms to the manuscript.

Registry No. hCT, 21215-62-3; DMSO, 67-68-5; L-Pro, 147-85-3; water, 7732-18-5.

References

Austin, L. A., & Heath, H. (1981) *N. Engl. J. Med 304*, 269–278.

Bax, A., & Davis, D. (1985) *J. Magn. Reson. 65*, 355–366.
Billeter, M., Braun, W., & Wüthrich, K. (1982) *J. Mol. Biol. 155*, 321–346.
Bodenhausen, G., Vold, R. L., & Vold, R. R. (1980) *J. Magn. Reson. 37*, 93–106.
Brandl, C. J., & Deber, C. M. (1986) *Proc. Natl. Acad. Sci. U.S.A. 83*, 917–921.
Brandts, J. F., Halvorson, H. R., & Brennan, M. (1975) *Biochemistry 14*, 4953–4963.
Braunschweiler, L., & Ernst, R. R. (1983) *J. Magn. Reson. 53*, 521–528.
Briggs, M. S., & Gierasch, L. M. (1986) *Adv. Protein Chem. 38*, 109–180.
Briggs, M. S., Cornell, D. G., Dluhy, R. A., & Gierasch, L. M. (1986) *Science 233*, 206–208.
Chazin, W. J., Hugli, T. E., & Wright, P. E. (1988) *Biochemistry 27*, 9139–9148.
Chazin, W. J., Kördel, J., Drakenberg, T., Thulin, E., Brodin, P., Grundström, T., & Forsén, S. (1989) *Proc. Natl. Acad. Sci. U.S.A. 86*, 2195–2198.
Davis, D. G., & Bax, A. (1985) *J. Magn. Reson. 64*, 533–538.
Dayhoff, M. O. (1978) *Atlas of Protein Sequence and Structure*, National Biomedical Research Foundation, Silver Spring, MD.
Doi, M., Yamanaka, Y., Kobayashi, Y., Kyogoku, Y., Takimoto, M., & Gota, K. (1989) *Proceedings of the 11th American Peptide Symposium*, LaJolla, CA (Rivier, J. E., & Marshall, G. R., Eds.) p 45.
Douzou, P., & Petsko, G. A. (1984) *Adv. Protein Chem. 36*, 245–361.
Drobny, G., Pines, A., Sinton, S., Weitkamp, D., & Wemmer, D. (1979) *Faraday Div. Chem. Soc. Symp. 13*, 49–55.
Dwek, R. (1973) *Nuclear Magnetic Resonance in Biochemistry*, Oxford University Press, London.
Eich, G., Bodenhausen, G., & Ernst, R. R. (1982) *J. Am. Chem. Soc. 104*, 3731–3732.
Epand, R. M. (1983) *Mol. Cell. Biochem. 57*, 41–47.
Epand, R. M., Epand, R. F., Orlowski, R. C., Schleuter, R. J., Boni, L. T., & Hui, S. W. (1983) *Biochemistry 22*, 5074–5084.
Epand, R. M., Epand, R. F., & Orlowski, R. C. (1985) *Int. J. Pept. Protein Res. 25*, 105–111.
Epand, R. M., Epand, R. F., Orlowski, R. C., Seyler, J. K., & Colescott, R. L. (1986a) *Biochemistry 25*, 1964–1968.
Epand, R. M., Stahl, G. L., & Orlowski, R. C. (1986b) *Int. J. Pept. Protein Res. 27*, 501–506.
Epand, E. M., Epand, R. F., & Orlowski, R. C. (1988) *Biochem. Biophys. Res. Commun. 152*, 203–207.
Fesik, S. W., & Olejniczak, E. T. (1987) *Magn. Reson. Chem. 25*, 1046–1048.
Findlay, D. M., Michaelangeli, V. P., Orlowski, R. C., & Martin, T. J. (1983) *Endocrinology 112*, 1288–1291.
Fink, A. L. (1986) *Methods Enzymol. 131*, 173–185.
Fisher, J. A., Tobler, P. H., Kaufman, M., Born, W., Henke, H., Cooper, P. E., Sagar, S. M., & Martin, J. B. (1981) *Proc. Natl. Acad. Sci. U.S.A. 78*, 7801–7805.
Gierasch, L. M., Lacy, J. E., Thompson, K. F., Rockwell, A. L., & Watnick, P. I. (1982) *Biophys. J. 37*, 275–284.
Grathwohl, C., & Wüthrich, K. (1981) *Biopolymers 20*, 2623–2633.
Hetzel, R., & Wüthrich, K. (1979) *Biopolymers 18*, 2589–2606.
Jeener, J., Meier, B. H., Bachmann, P., & Ernst, R. R. (1979) *J. Chem. Phys. 71*, 4546–4553.
Kördel, J., Forsén, S., Drakenberg, T., & Chazin, W. J. (1990) *Biochemistry 29*, 4400–4409.
Llinás, M., & Klein, M. P. (1975) *J. Am. Chem. Soc. 97*, 4731–4737.
Lolkema, J. S., Püttner, I. B., & Kaback, H. R. (1988) *Biochemistry 27*, 8307–8310.
Macura, S., & Ernst, R. R. (1980) *Mol. Phys. 41*, 95–117.
Moe, G. R., & Kaiser, E. T. (1985) *Biochemistry 24*, 1971–1976.
Moe, G. R., Miller, R. J., & Kaiser, E. T. (1983) *J. Am. Chem. Soc. 105*, 4100–4102.
Motta, A., Picone, D., Tancredi, T., & Temussi, P. A. (1987) *J. Magn. Reson. 75*, 364–370.
Motta, A., Picone, D., Tancredi, T., & Temussi, P. A. (1988) *Tetrahedron 44*, 975–990.
Motta, A., Castiglione-Morelli, M. A., Goud, N., & Temussi, P. A. (1989) *Biochemistry 28*, 7998–8002.
Otting, G., Widmer, H., Wagner, G., & Wüthrich, K. (1986) *J. Magn. Reson. 66*, 187–193.
Otting, G., Qian, Y., Müller, M., Affolter, M., Gehring, W., & Wüthrich, K. (1988) *EMBO J. 7*, 4305–4309.
Pardi, A., Billeter, M., & Wüthrich, K. (1984) *J. Mol. Biol. 180*, 741–751.
Piantini, U., Sørensen, O. W., & Ernst, R. R. (1982) *J. Am. Chem. Soc. 104*, 6800–6801.
Richardson, J. S. (1981) *Adv. Protein Chem. 34*, 167–339.
Rizzo, A. J., & Goltzman, D. (1981) *Endocrinology 108*, 1672–1677.
Sargent, D. F., & Schwyzer, R. (1986) *Proc. Natl. Acad. Sci. U.S.A. 83*, 5774–5778.
Schichman, S. A., & Amey, R. L. (1971) *J. Phys. Chem. 75*, 98–102.
Schmid, F. X., & Baldwin, R. L. (1978) *Proc. Natl. Acad. Sci. U.S.A. 75*, 4764–4768.
Smith, J. A., & Pease, L. G. (1986) *Crit. Rev. Biochem. 8*, 315–380.
Tobias, B., & Markley, J. L. (1986) *J. Magn. Reson. 69*, 381–385.
Wagner, G., Neuhaus, D., Wörgötter, E., Vasak, M., Kägi, J. R. H., & Wüthrich, K. (1986) *J. Mol. Biol. 187*, 131–135.
Wüthrich, K. (1976) in *NMR in Biological Research: Peptides and Proteins*, pp 65–72, North-Holland, Amsterdam.
Wüthrich, K. (1986) *NMR of Proteins and Nucleic Acids*, J. Wiley & Sons, New York.
Wüthrich, K., Billeter, M., & Braun, W. (1984) *J. Mol. Biol. 180*, 715–740.
Zuiderweg, E. R. P., Hallenga, K., & Olejniczak, E. T. (1986) *J. Magn. Reson. 70*, 336–343.